Finite Element Model of a Self-Oscillating IPMC

Deivid Pugal*
Active Materials and Processing Laboratory,
Mechanical Engineering Department,
University of Nevada, Reno, U.S.A and
IMS Lab, Institute of Technology, Tartu University, Estonia

Kwang J. Kim†
Active Materials and Processing Laboratory,
Mechanical Engineering Department,
University of Nevada, Reno, U.S.A

Andres Punning, Heiki Kasemägi, Maarja Kruusmaa, and Alvo Aabloo
IMS Lab, Institute of Technology, Tartu University, Estonia
(Dated: June 2, 2007)

This paper presents a electro-mechanical model of an ionic polymer-metal composite (IPMC) material. The technique of the modelling is Finite Element method (FEM). An applied electric field causes the drift of counter-ions (e.g. Na+) which in turn drags water molecules along. The mass and charge imbalance inside the polymer is the main cause of the bending motion of the IPMC. All foregoing physical effects have been considered as time dependent and modelled with FEM. The model takes into account the mechanical properties of Nafion polymer as well as thin coating of the platinum electrodes. (Furthermore, the water drift and the counter ion drift inside the polymer backbone is considered separately.) As self-oscillating behavior of an IPMC was described in our previous paper, the modelling of the electrochemical reactions is also considered. Reactions occuring on the surface of the platinum electrode, which is immersed into formaldehyde (HCHO) solution, are described by partial differential equations and also modeled using FEM. By coupling the equations to the rest of the model, we are able to simulate self-oscillatory behavior of an IPMC sheet.

I. INTRODUCTION

Electroactive polymer (EAP) based materials are valuable for many applications from micro robotics to military and space applications. Some of the advantages of EAP materials are light weight, noiseless actuation, simple mechanics and large displacement. In addition some EAPs, such as IPMCs [1], are able to function in aquous environments. Those qualities make the materials possible to use as artificial muscles. In this paper we consider simulations of IPMC type materials with the Finite Element method.

IPMC materials are highly porous polymer materials such as Nafion^{TM}, Teflon, filled with some kind of ionic conductive liquid. There are water based IPMCs which operate in aquatic environment and current is caused by ions such as Na+, K+ dissociated in water. Other kind of IPMCs - ionic liquid based, do not need wet environment for operating. A sheet of an ionic polymer is coated with a thin metal layer, usually platinum or gold. All freely movable cations inside the polymer migrate towards an electrode due to applied electric field, causing expansion of the material at the one end of the sheet and contraction at the other end, which results in bending of the sheet.

For simulating actuation of an IPMC sheet we need to solve coupled problems due to the complex nature of bending of an IPMC. It includes simulations in different domains such as mechanical, electrostatic and mass transfer, and even electrochemical for more advanced models. Some authors [2, 3] have already simulated mass transfer and electrostatic effects. We have used similar approach in our model. Toi [4] has shown a Finite Element model including viscocity terms in transportation processes explicitly. However, the basis of the described model is a rectangular beam with 2 pairs of electrodes. Our approach for simulating mechanical bending is taking advantage of the numerical nature of FEM problems - we use continuum mechanics equations instead of analytical Euler beam theroy which is more commonly used by authors [5, 6]. By coupling equations from different domains, we get a model for an IPMC muscle sheet, which allows us to use it as a starting point for solving more complex problems, thus we have introduced a simulation of electrochemical reactions on the platinum electrode of an IPMC sheet, which leads to self-oscillating actuation. Spontaneous oscillations are common phenomena in nature and have been studied in many experiments, including electrochemical systems such as oxidation of organic materials and metals [7]. Under certain conditions such system can generate oscillations [8]. We have conducted a series of tests, where an IPMC sheet have been immersed into acidic formaldehyde (HCHO) solution and exposed to a constant potential. The measurements,

---

*Electronic address: david@ut.ee
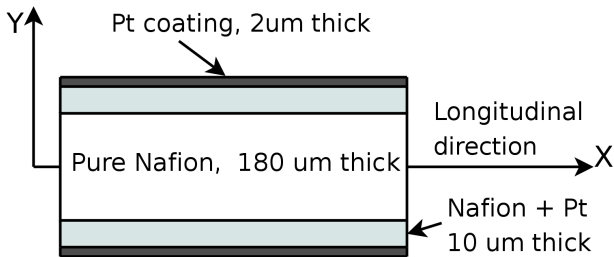†Electronic address: kwangkim@unr.edu

Figure 1: Illustration of domains and dimensions used in simulations. Notice that there are three different mechanical domains - pure Nafion^{TM} polymer, pure Pt coating and diffusion layer, where Pt has diffused into the polymer.

however show current oscillations, which in turn result in oscillating bending of the IPMC sheet [9]. Hence we have introduced a FEM model in this paper to describe time dependent bending of a self-oscillating IPMC.

II. BENDING SIMULATION DETAILS

An IPMC sheet consists of a polymer host and a metal coating. In our experiments, we have used Nafion^{TM} 117, coated with thin layer of platinum. Mass transfer and electrostatic simulations are done in three mechanical domains: pure backbone polymer, pure platinum coating, and mixture of polymer and platinum - some platinum tends to diffuse into the polymer during coating process [10]. Physical properties and dimensions of pure, 2 μm thick platinum coating are considered only when calculating bending. That gives us five mechanical domains as shown in Fig. 1. Most simulations are carried out for an IPMC strip, 2-4 cm long, 200 μm thick polymer, including 10 μm thick Pt diffusion region on each side, coated with 2 μm thick platinum, in a cantilever configuration - one end of the strip is fixed.

The Nernst-Planck equation describes diffusion, convection and in presence of electric field and charges, migration of the particles. The general form of the equation is

$$\frac{\partial C}{\partial t} + \nabla \cdot (-D\nabla C - z\mu FC\nabla\phi) = -\vec{u} \cdot \nabla C, \quad (1)$$

where C is concentration, D diffusion constant, F Faraday constant, $\vec{u}$ velocity, z charge number, ϕ electric potential, and μ mobility of species, which is found by using known relation $\mu = D/(RT)$. The variable T is absolute temperature and R universal gas constant. Movable counter ions are described by Eq. (1). As anions are fixed, they maintain constant charge density throughout the polymer. After a voltage is applied to the electrodes of an IPMC, all free cations will start migrating towards cathode, causing current in the outer electric circuit. Because of the fact that ions cannot move beyond the boundary of the polymer, charges start to accumulate, resulting in increase of the electric field, which cancels out the applied
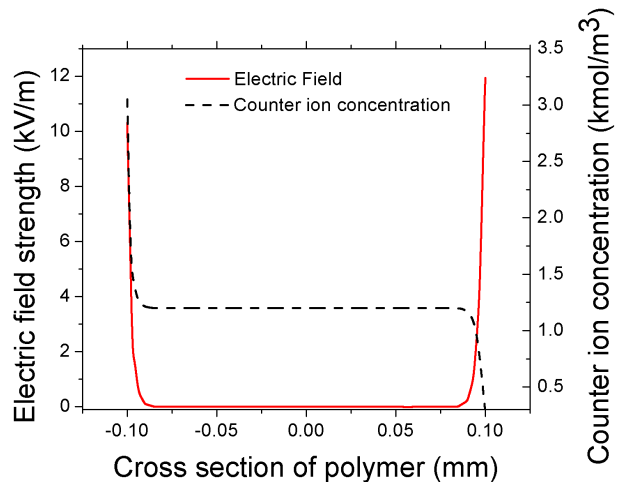

Figure 2: The concentration of counter ions and electric field strength inside the polymer according to simulations.

one. The process could be described by Gauss' Law:

$$\nabla \cdot \vec{E} = -\Delta\phi = \frac{F \cdot \rho}{\varepsilon}, \quad (2)$$

where ρ is charge density, ε is absolute dielectric constant and E is the strength of the electric field. A steady state of the cations forms when electric field created by distribution of cations cancels out the applied electric field, i.e. the strength of the electric field inside the polymer is approximately zero, as also shown in Fig. 2. The steady state cation concentration, with average value of 1200 mol/m^3 is also shown in the same figure. It is interesting to notice that there are fluctuations in charge distribution only in really thin boundary layers, leading to the conclusion that there is no charge imbalance inside the polymer. General understanding is that locally generated charge imbalance nearby platinum electrodes is directly connected, and mainly responsible, to the bending of an IPMC [11]. Therefore we define longitudinal force per unit area at each point in the polymer of an IPMC as follows [6]:

$$\vec{F} = (A\,\rho + B\,\rho^2)\,\hat{x}, \quad (3)$$

where ρ is charge density and A and B are constants which could be found from different experiments. Values of the constants are brought out in Table II and it is interesting to notice that the ratio A/B is close to the value suggested by Wallmersperger [6]. Equations (1)-(3) are described only for pure Nafion^{TM} and Pt diffusion domain (see Fig. 1). There are no ion diffusion nor migration in thin Pt coating domain.

To relate the force in Eq. 3 to the physical bending of an IPMC sheet, we introduce a set of continuum mechanics equations, which are effective in all domains

Table I: Material parameters used in continuum mechanics equations.

Parameter	Value	Unit	Domain where applied
E_N	200	MPa	Nafion^{TM}
ν_N	0.49	-	Nafion^{TM}
E_{Pt}	168	GPa	Pt
ν_{Pt}	0.38	-	Pt
E_{diff}	84	GPa	Pt diffusion layer (estimated)
ν_{diff}	0.42	-	Pt diffusion layer (estimated)

Table II: Parameter values used in bending simulations.

Parameter	Value	Unit
D	1×10^{-6}	cm^2/s
R	8.31	$J/(K\ mol)$
T	293	K
z	1	$-$
F	96.5×10^6	mC/mol
ε	25	mF/m
A	110	$N\ m/mol$
B	12	$N\ m^4/mol^2$
$\alpha_{polymer}$	0	s^{-1}
$\beta_{polymer}$	1.5	s

(Fig. 1). These equations are described in Comsol Multiphysics structural mechanics software package. Normal and shear strain are defined as

$$\varepsilon_i = \frac{\partial u_i}{\partial x_i},\ \varepsilon_{ij} = \frac{1}{2}\left(\frac{\partial u_i}{\partial x_j} - \frac{\partial u_j}{\partial x_i}\right), \quad (4)$$

where u is the displacement vector, x denotes a coordinate and indices i and j are from 1 to 3 and denote components correspondingly to x, y, or z direction. The stress-strain relationship is

$$\sigma = D\varepsilon, \quad (5)$$

where D is 6×6 elasticity matrix, consisting of components of Young's modulus and Poisson's ratio. The system is in equilibrium, if the relation

$$-\nabla \cdot \sigma = \vec{F}, \quad (6)$$

is satisfied. This is Navier's equation for displacement. The values of Young's modulus and Poisson's ratios, which are used in the simulations, are shown in Table I. The values for platinum diffusion region are not measured, but estimated as an average of values of pure Nafion^{TM} and Pt region.

As our simulations are rather dynamic than static, we have to introduce an equation to describe the motion of an IPMC sheet. To do that, we use Newton's Second law

$$\rho\frac{\partial^2 \vec{u}}{\partial t^2} - \nabla \cdot c\nabla\vec{u} = \vec{F}, \quad (7)$$
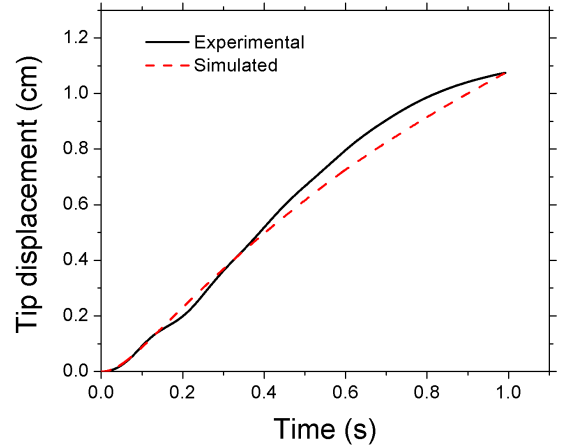

Figure 3: Experimental and simulation results of tip displacement. Although there is a slight difference of graphs in large displacement region, the model gives precise estimation for smaller displacement.

where the second term is the static Navier's equation. The first term in Eq. (7) introduces the dynamic part. Several authors have reached to the conclusion that IPMC materials exhibit viscoelastic behavior [12, 13], which is especially noticable for high frequency movements [14]. However, we include the viscoelastic term in our equations by means of using Rayleigh damping [15] model, which is described for a system of one degree of freedom as follows:

$$m\frac{d^2u}{dt^2} + \xi\frac{du}{dt} + ku = f(t), \quad (8)$$

where the damping parameter ξ could be expressed as $\xi = \alpha m + \beta k$. The parameter m is a mass, k is a stiffness and α and β are correspondingly damping coefficients. The equation for the multiple degrees of freedom is

$$\rho\frac{\partial^2 \vec{u}}{\partial t^2} - \nabla \cdot \left[c\nabla\vec{u} + c\beta\nabla\frac{\partial\vec{u}}{\partial t}\right] + \alpha\rho\frac{\partial\vec{u}}{\partial t} = \vec{F}. \quad (9)$$

By coupling Eq. (9) to the previously described equations, a good basic model for IPMC actuation has been got. The damping equation turned out to be very necessary to describe correct movement of an IPMC strip. Though the values of the parameters α and β are empirical (see Table II), they have an important role of improving the dynamical behavior of the model for non-constant applied voltages.
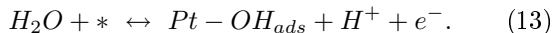
All values, which are used in the simulations, have been brought out in Table II. Fig. 3 shows a comparison between the simulation and an experiment [16]. More comparative figures are introduced in the next section of the paper.

III. MODELING SELF-OSCILLATIONS

We have conducted a series of tests with IPMCs in a constant electric field in formaldehyde (HCHO) solution. Measurements show that current oscillations begin from applied potential of ca. 0.75 V. More information about experiments and conclusions could be read from our previous letter [9]. Studies show that there are sequential electrochemical reactions, which take place on the platinum cathode. The initial burst of the current is caused by the reaction

$$CO_{ads} + OH_{ads} \rightarrow CO_2 + H^+ + e^- + 2*, \qquad (10)$$
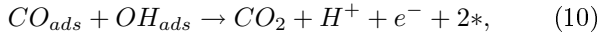
where subscript ads denotes species adsorbed to the platinum and $*$ denotes an active platinum site. The result of the reaction (10) is clearing up 2 platinum sites, which causes CO to adsorb again. Chronopotentiomentry scans show that before reaction (10), the following reactions occur:

$$HCHO + * \rightarrow Pt - CHO_{ads} + H^+ + e^-, \quad (11)$$
$$Pt - CHO \rightarrow Pt - CO_{ads} + H^+ + e^-, \qquad (12)$$
$$H_2O + * \leftrightarrow Pt - OH_{ads} + H^+ + e^-. \qquad (13)$$

HCHO is dissociated on the electrode surface at lower anodic potentials. Higher anodic potentials cause dehydrogenation of water which results in water oxidation with intermediate Pt-OH formation. We believe that these reaction lead to oscillating potentials, which in turn lead to self-oscillating motion of the IPMC sheet.

Series of chronopotentiometry scans were conducted to characterize oscillations for different HCHO concentration and current densities. As was brought out in our previous paper [9], the oscillations start at approximately 7 mA/cm^2. The experiments were conducted up to current density values of 40 mA/cm^2. Tests with HCHO concentrations of 1 M, 2 M, and 3 M show that oscillations frequencies remain constant up to the current density of 14 mA/cm^2, but after further increasing the current, in 1 M HCHO, the frequency decreases, in 2 M HCHO, the frequency remains constant, and in 3 M HCHO solution, the frequency starts to increase, as also shown in Fig. 4. Our goal is to develope a model for describing the frequency behavior depending on HCHO concentration and the current density. The basic model and concepts are taken from PhD thesis of D. Kim [17] and work of P. Strasser [18]. To describe the oscillations, four dynamic parameters, therefore four differential equations, must be observed: concentration of adsorbed OH, CO, the change of the double layer potential due to electrochemical reactions, and the change of the concentration of HCHO near the surface of platinum. First two variables could be expressed for a certain current density and HCHO concentration as [17]:

$$\dot{\theta}_{CO} = k_2 M - k_4 \theta_{CO} \theta_{OH}, \qquad (14)$$
$$\dot{\theta}_{OH} = k_3 \theta_{CO} M - k_{-3} \theta_{OH} - k_4 \theta_{CO} \theta_{OH}, \quad (15)$$
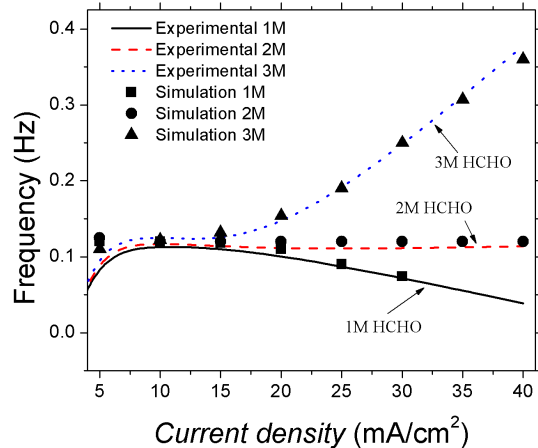

Figure 4: Experimental[9] and simulated frequency dependence on concentration of HCHO and applied current density. Simulations for 1 M HCHO concentration does not go past 30 mA/cm^2, because given equation system did not give reasonable results beyond that current density.

where θ_{CO} and θ_{OH} are normed adsorbtion coverages of CO and OH. Variables k_i and M are described by equations

$$k_i(\phi) = exp[s_i(\phi - \phi_i)], \qquad (16)$$
$$M = (1 - \theta_{CO} - \theta_{OH}), \qquad (17)$$

where s_i are modeling coefficients and ϕ_i are potentials of the reactions [17]. As our model is highly dynamic, the double layer with thickness δ near the platinum electrode is introduced. At the far end of the layer, the concentration of the formic acid is considered constant, and due to the adsorbtion of HCHO on Pt, the concentration of the solution is changing in time near the electrode. There are two components responsible of decrease of the concentration. The first one is direct oxidation of the formic acid to CO_2 and $2H^+$, the second one is adsorbtion of CO on the platinum surface due to electrochemical reactions [18]. The mechanism, which restores the HCHO concentration near the surface is diffusion. So the amount of the formic acid is decreasing significantly while the adsorption rate is high and increasing due to the diffusion during the low adsorbtion period. The equation describing the diffusion process is

$$\frac{\partial c_{FA}}{\partial t} = \nabla \cdot (D_{FA} \nabla c_{FA}) \qquad (18)$$

with constant concentration at the far end of the double layer and flux

$$f = k_2 M (1 + k c_r) \times S_{tot}, \qquad (19)$$

as boundary condition on the electrode. Here S_{tot} denotes the total number of platinum sites per surface

Table III: Variables and values used in the simulation of electrochemical oscillations.

Parameter	Value	Unit
S_{tot}	0.5×10^{-6}	mol/cm^2
C_{dl}	1	mF/cm^2
A	1.2	$cm^7 / \left(mA^2 \times mol\right)$
k	100	-
δ^a	3×10^{-2}	cm
$D_{FA}{}^a$	2.5×10^{-5}	cm^2/s
$\phi_{1,2,3,-3,4}{}^b$	[0.2, 0.3, 0.01, 0.512, 0.77]	V
$s_{1,2,3,-3,4}{}^b$	[10, −11, 9, −9, 20]	V^{-1}

[a]Ref. [18]
[b]Ref. [17]

area, c_r is normed concentration near boundary layer and equals $c_r = c_{FA}/c_0$, where c_0 is an initial concentration. Variable k is a simulation constant. The second term of Eq. (19) represents simplified version of the direct oxidation path [18]. Considering those equations and interesting nature of frequency characteristic for different amounts of HCHO (Fig. 4), we can now describe somewhat empirical, gray box [19] equation for the last dynamic variable - the double layer potential:

$$\dot{\phi} = \frac{1}{C_{dl}} \left[j_{th} - j_d + A \times B \times j^2 \times (j - j_{th}) \times c_r - \right.$$
$$\left. - S_{tot} F \left(k_1 M + k_4 \theta_{CO} \theta_{OH} \right) \right], \quad (20)$$

where j is applied current density, j_{th} is threshold current density with approximate value of 10 mA/cm^2, j_d is direct current density and is proportional to the second term of Eq. (19). The variable B could be explicitly written as $B = c_0 - c_{neutral}$, where $c_{netural}$ corresponds to the concentration of 2 M. This is denoted "netural" concentration, because as could be seen in Fig. 4, the oscillation frequency for the case $c_0 = c_{neutral} = 2\ M$ does not depend on the applied current density. The numeric data could be found in Table III. The third term in Eq. (20) is empirical and reflects the interesting behavior of the oscillations frequency for different formic acid concentrations. Other terms are similar to the ones described by Strasser [18]. However, some values are adjusted to get realistic simulation results. Measured voltage oscillation comparison to simulation data could be seen in Fig. 5.

By using the obtained voltage output in the base Finite Element Model, which is described in the previous section, we can simulate oscillating deflection of an IPMC muscle. Two sample results for different HCHO concentrations and current densities are shown in Figures 6 and 7. As it could be seen, the amplitude, frequency and for the most part, shape of the deflection show reasonable agreement between modeling and experimental data. However, there is some disharmony at the areas of maximum deflection, where the experiments show really sharp deflections in comparison to rather smooth simulation results.
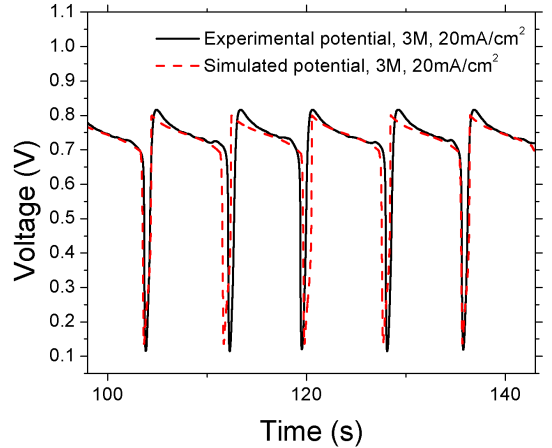

Figure 5: Potential oscillations. Measured data[17] and simulated data for 3M HCHO solution, with applied current density of 20 mA/cm^2.
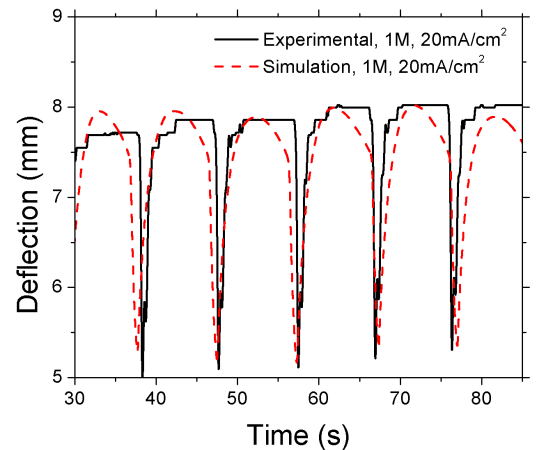

Figure 6: Oscillating tip displacement. Experimental[17] data and simulation data for 1M solution, applied current density of 20 mA/cm^2.

IV. SUMMARY AND CONCLUSIONS

We have developed a Finite Element model for simulating actuation of an IPMC. The model is largely based on physical quantities and well known or measurable variables. The migration and diffusion of the counter ions inside the Nafion^{TM} polymer is described along the electric field change due to the charge imbalance. This in turn is tied in to continuum mechanics and dynamics equations, forming a complete system of equations to describe the bending of an IPMC sheet.

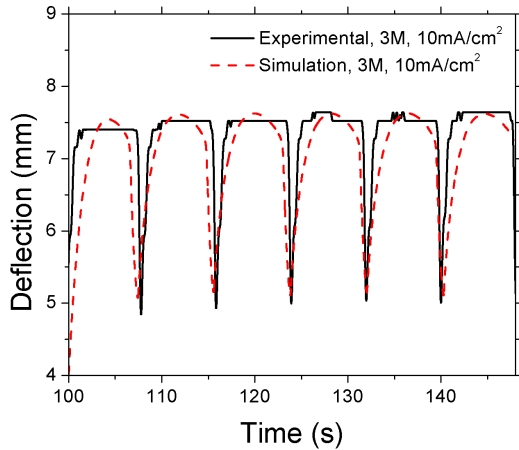The comparison of experimental and simulated tip dis-

ture of the IPMC. Taking into account the surrounding environment of the IPMC could also improve the results.

The second part of the work describes the extended model for self-oscillating IPMCs. The oscillations occur when a platinum coated IPMC is immersed into formic acid solution and subjected to a constant potential or current. The extended model takes into account formic acid concentration changes near the electrode and poisoning level of the platinum sites. This in turn results in the oscillating double layer potential, which is used in the base model for calculating time dependent tip displacement of the IPMC muscle. For the most part, the model follows simulation data closely. However, the experimental deflection shows some very sharp movements at certain regions, but the simulation gives rather smooth displacement profiles. The future work includes studying further this interesting behavior and possibly improving the model.

Figure 7: Oscillating tip displacement. Experimental[17] data and simulation data for 3M solution, applied current density of 10 mA/cm^2.

placement in time shows reasonable agreement, especially for smaller deflections. The future work is getting simulations more precise for large displacements, possibly including equations, which describe voltage distribution on the surface of the electrdodes depending on the curva-

[1] M. Shahinpoor and K. J. Kim, Smart Materials and Structures **10**, 819 (2001), ISSN 0964-1726.

[2] T. Wallmersperger, B. Kroplin, and R. W. Gulch, Mechanics of Materials **36**, 411 (2004), ISSN 0167-6636.

[3] S. Nemat-Nasser and S. Zamani, Journal of Applied Physics **100** (2006), ISSN 0021-8979.

[4] Y. Toi and S.-S. Kang, Computers and Structures **83**, 2573 (2005), ISSN 0045-7949.

[5] S. Lee, H. C. Park, and K. J. Kim, Smart Materials and Structures **14**, 1363 (2005), ISSN 0964-1726.

[6] T. Wallmersperger, D. J. Leo, and C. S. Kothera, Journal of Applied Physics **101** (2007), ISSN 0021-8979.

[7] B. Miller and A. Chen, Journal of Electroanalytical Chemistry **588**, 314 (2006), ISSN 0022-0728.

[8] K. Krischer, Journal of Electroanalytical Chemistry **501**, 1 (2001), ISSN 0022-0728.

[9] D. Kim, K. J. Kim, Y. Tak, D. Pugal, and I.-S. Park, Applied Physics Letters **90** (2007), ISSN 0003-6951.

[10] S. Nemat-Nasser and Y. Wu, Journal of Applied Physics **93**, 5255 (2003), ISSN 0021-8979.

[11] S. Nemat-Nasser and J. Y. Li, Journal of Applied Physics **87** (2000), ISSN 0021-8979.

[12] K. M. Newbury and D. J. Leo, Journal of Intelligent Material Systems and Structures **14**, 333 (2003), ISSN 1045-389X.

[13] K. Yagasaki and H. Tamagawa, Physical Review E - Statistical, Nonlinear, and Soft Matter Physics **70**, 052801 (2004), ISSN 1539-3755.

[14] K. M. Newbury and D. J. Leo, Journal of Intelligent Material Systems and Structures **14**, 343 (2003), ISSN 1045-389X.

[15] R. Lord, New York, Dover **2**, 226 (1945).

[16] A. Punning, M. Kruusmaa, and A. Aabloo, Sensors and Actuators, A: Physical **133**, 200 (2007), ISSN 0924-4247.

[17] D. Kim, Ph.D. thesis, University of Nevada (2006).

[18] P. Strasser, M. Eiswirth, and G. Ertl, Journal of Chemical Physics **107** (1997), ISSN 0021-9606.

[19] M. Shahinpoor and K. J. Kim, Smart Materials and Structures **13**, 1362 (2004), ISSN 0964-1726.